Characterization of new recombinant Immunoglobulins type-M binding to C1q by Biolayer Interferometry

Anne Chouquet[a], Andrea J. Pinto[a], Wai Li Ling[a], Julia Hennicke[b], Isabelle Bally[a], Linda Schwaigerlehner[b], Nicole M. Thielens[a], Renate Kunert[b], Jean-Baptiste Reiser[a*]

[a]*Institut de Biologie Structurale, UMR 5075, Univ. Grenoble Alpes, CEA, CNRS, IBS, F-38000 Grenoble, France;* [b]*Department of Biotechnology, University of Natural Resources and Life Sciences, Muthgasse 18, 1190 Vienna, Austria*

[*]Correspondance to: Jean-Baptiste Reiser, Institut de Biologie Structurale, UMR 5075, Univ. Grenoble Alpes, CEA, CNRS, IBS, F-38000 Grenoble, France, E-mail: jean-baptiste.reiser@ibs.fr; Work telephone number: +33 (0)4 57 42 95 49

Word count: 7345

Characterization of new recombinant Immunoglobulins type-M binding to C1q by Biolayer Interferometry

The Immunoglobulins type-M (IgMs) are one of the first antibody classes mobilized during immune responses against pathogens and tumor cells. Binding to specific target antigens enables the interaction with the C1q complex which strongly activates the classical complement pathway. This biological function is the base for the huge therapeutic potential of IgMs but due to their high oligomeric complexity, *in vitro* production as well as biochemical and biophysical characterizations are challenging. In the present study, we present new attempts of recombinant production of two IgM models (IgM617 and IgM012) and the evaluation of their polymer distribution using biophysical methods (AUC, SEC-MALLS, Mass Photometry, transmission EM). Each IgM has an individual specific expression yield with different protein quality likely due to intrinsic IgM properties and patterning. Despite the presence of additional oligomeric states, purified recombinant IgMs retain their ability to activate complement in a C1q dependent manner. More importantly, a new method to evaluate their functional quality attribute by characterizing the kinetics of C1q binding to recombinant IgM has been developed using BioLayer Interferometry (BLI). We show that recombinant IgMs possess similar C1q binding properties as IgMs purified from human plasma.

Keywords: IgM, immunoglobulins, complement, C1q, recombinant expression, biophysical characterization, protein-protein interactions, biolayer interferometry

Introduction

Since their discovery over a century ago, immunoglobulins (Igs) are considered to be one of the main parts of the vertebrate humoral immune responses representing the first line of host protection against pathogens and altered-self cells, immune surveillance and homeostasis by recognizing and binding specific antigens. Immunoglobulins of type M (IgMs) are the first Igs produced and secreted by B cells in early infection and immune reaction stages in adults. They are highly oligomeric glyco-polypeptides composed of a heavy chain (H) and a light chain (L). Each chain contains an N-terminal variable domain and one (for the L chain) or four (for the H chain) C-terminal constant domains. IgMs are found as assembly of H_2L_2 protomer subunits

either in a pentameric form $(H_2L_2)_5$, containing an additional covalently linked peptide called the Joining (J) chain or, to a minor extend (less than 5%), in hexameric form $(H_2L_2)_6$, devoid of J chain (for reviews see refs. 1–3). The overall assembly of IgMs is now revealed by modern high resolution Electron Microscopy (EM) methods: they have been observed as star-shaped structures with a compact Fc core and orbiting, labile and flexible Fab arms. While the hexamers appear with the expected 6-fold symmetry, the pentamers possess a pseudo-hexameric symmetry where five IgM protomers occupy five of the six symmetric positions and the J chain the sixth position.[4–6]

In addition to their antigen recognition function, IgMs fulfil their immune effector function as one of the strongest activators of the classical pathway of the complement system. The binding of complexes between specific surface-exposed antigens and IgMs to the first recognition component of the classical pathway (CP), the C1q molecule, initiates complement-dependent cytotoxicity, a regulated amplifying, amplifying proteolytic cascade which enable the membrane attack complex formation and the elimination of the pathogen or infected cell targets.[7,8] Found in high concentration in human serum, C1q, which forms the CP initiation C1 complex together with the pro-enzyme tetramer $C1r_2C1s_2$, is a 460kDa and highly flexible glycoprotein assembled from 18 polypeptide chains of 3 types (A, B, C). It is organized into six ABC heterotrimers forming six Ig recognition domains, the globular heads (gC1q), attached to collagen-like regions (CLR) allowing the assembly of what has been depicted as a “bouquet of tulips” or an “Eiffel-tower”.[9–11]

Interaction studies of C1q with its Ig ligands led to the recent Ig/C1 complexes structures by cryo-electron tomography and microscopy that finally revealed the general assembly of the CP initiation step and confirmed some, but not all, of the different biochemical studies performed to characterize the C1q/Ig binding properties and to identify the C1q/Ig binding sites.[11,12] But, studies to evaluate the direct binding characteristics of C1q to Igs are rather limited in number

to evaluate complement function and activation and to use them as methods to evaluate the quality attributes (reviewed in ref. 13). Traditional methods employ Enzyme-Linked Immunosorbent Assays (ELISA) to measure equilibrium and end-point deposition of Igs over coated C1q and vice-et-versa (exemplified in refs. 14,15). More recently, label-free and real-time methods such as traditional Surface Plasmon Resonance (SPR) or novel BioLayer Interferometry (BLI) have been used to characterize the binding kinetics between C1q and IgGs[16–18] or IgMs[19].

In the present study, we report (i) new recombinant production of our IgM models, IgM617 and IgM012 (ii) their biochemical and functional quality characterization using Analytical UltraCentrifugation (AUC), Size Exclusion Chromatography coupled to Multi-Angle Laser Light Scattering (SEC-MALLS), Mass Photometry (MP), Transmission Electron Microscopy (TEM) and in-house ELISA-like for detection of complement activation and (iii) the development of protocols to evaluate their bindings to C1q with BLI and to compare their kinetics characteristics.

Results

Expression and purification of new recombinant IgM forms produced by HEK293F

Previously, the production of recombinant IgM models using different mammalian expression systems was intensively studied in stable and transient expression.[20–26] Here, we present an additional production system for the two IgM constructs, IgM617 and IgM012, using stabilized HEK293F cell lines. cDNA of H, L and J chains from both models have been individually subcloned in pcDNA3.1(+). HEK293F cells were transfected either with the three pcDNA3.1(+) constructs or with only H and L vector constructs with the attempt to obtain IgM samples in pentameric forms (IgM617-HLJ and IgM012-HLJ) or in hexameric forms (IgM617-HL and IgM012-HL), respectively. After selection and culture expansion, recombinant IgMs

were purified from culture media using the optimized protocol established by Hennicke *et al.*.[20] The retrieved yields and sample qualities after purification differ from one recombinant IgM to the other with higher product titers for IgM617. Indeed, the final purified yield from stable HEK293F culture media of IgM617-HLJ or IgM617HL (5 to 10 mg/l of culture supernatant) is 25 to 100 times higher than that of IgM012-HLJ or IgM012-HL (less than 0.1 mg/l of culture supernatant). The production, yield and sample quality of IgM617 appear reproducible from different cell cultivations and are far more variable for IgM012s and often, samples suffer from low amounts of product and quality homogeneity.

Oligomeric distribution of new recombinant IgM forms produced by HEK293F

The oligomeric distribution and quality of purified IgM samples expressed by HEK293F cell lines were investigated with biochemical, biophysical and structural methods when feasible.

SDS-PAGE

Semi-native PolyAcrylamide Gel Electrophoresis (PAGE) adapted from Vorauer *et al.*[23] shows that purified IgM617-HLJ migrates as a single and homogeneous band while IgM617-HL migrates in a more heterogenous manner with two major bands in the highest molecular weight range (Figure 1a). Interestingly, and while IgM012-HLJ and IgM012-HL behave similarly to IgM617 constructs, noticeable additional bands at molecular weights below 150 kDa are still observed, suggesting the presence of lower oligomeric states (Figure 1b) similarly as it has been observed by Chromikova *et al.*[25] and Hennicke *et al.*[22] for the production of IgM617 and IgM012 pentamers in CHO DG44 or HEK239E cell lines.

SEC-MALLS and AUC

To further characterize IgM617-HLJ and IgM617-HL homogeneities, Multi-Angle-Light Scattering coupled to Size Exclusion Chromatography (SEC-MALLS) and sedimentation velocity Analytical Ultra-Centrifugation (sv-AUC) were performed.

First, SEC-MALLS analyses gave a homogeneous sharp peak of about 895 kDa for IgM617-HLJ (Supplemental Figure S1, panel b) which fall in the range of theoretical mass (pentamer peptide mass 891 kDa + 10 to 15% glycosylation). Surprisingly, a single mass of 950 kDa is also observed for IgM617-HL (Supplemental Figure S1 panel a), while the construct was anticipated by SDS-PAGE analysis to be a mixture of pentamers and hexamers. The observed mass may likely correspond to average molecular weights from the different glycosylated oligomers (hexamer peptide mass 1050 kDa; pentamers without J chain peptide mass 875 kDa + 10 to 15%). They might thus co-elute as a single peak from SEC and the resolution of this method is not sufficient to separate both hexamers and pentamers. To further explore sample heterogeneities, sv-AUC experiments were performed. Migration in the velocity field of IgM617-HLJ samples showed one main homogeneous peak at a sedimentation coefficient of about 19 S (more than 75 %) and minor peaks at 12 S (12 %) and 6 S (9 %), revealing the presence of a majority of pentamers but also presence of lower molecular weight oligomers (Supplemental Figure S2 panel b). Migration of IgM617-HL samples appeared to be even more heterogenous with two main peaks at about 21 S (between 60 to 70 % depending of lots) and about 17.5 S (25 to 30 %), which both may correspond to hexamers and pentamers, respectively; and two minor peaks at 15.0 S (5 %) and below 5 S (3 to 10 %), also lower molecular weight oligomers (Supplemental Figure S2 panel a). Our AUC data on recombinant IgMs are perfectly in agreement with the sedimentation coefficients originally measured by Eskeland *et al.* in 1975[27] on purified IgM from patient sera with or without J chain.

Mass Photometry

To further assess their oligomeric states and experimental molecular masses, IgM samples were analyzed using the emerging technique enabling accurate native mass measurements of single molecules in solution, the Mass Photometry (MP)[28]. A single population with an average mass of 998 +/- 6 kDa (mean +/- SD over replicates) can be observed for IgM617-HLJ (Figure 2b). The experimental mass matches the mass of fully glycosylated pentamers (theoretical peptide mass 891 kDa + 10 to 15% glycosylation). By contrast, IgM617-HL data show several mass populations: 3 main population at 1250 +/- 54 kDa, 1050 +/- 43 kDa, and 841 +/- 37 kDa (Figure 2a) that may correspond to hexamers (theoretical peptide mass 1050 kDa + 10 to 15% glycosylation), pentamers without J chain (875 kDa + 10 to 15%) and tetramers (700 kDa + 10 to 15%), respectively. Minor populations can also be observed and might correspond to lower oligomeric protomer states. This is in agreement with our sv-AUC observation of a mixture of IgM617-HL oligomers. However, the oligomeric distributions appear different and might be accountable for by the usage of different lots of IgM617-HL for the measurements but also by the methods used. IgM012-HLJ appears with a quite homogeneous experimental mass of 944 +/- 32 kDa, likely corresponding to pentamers (878 kDa + 10 to 15%) although the broad mass distribution is still observed and an additional population at low molecular weight is present and may correspond to the lower oligomeric states (Figure 2d). Finally, IgM012-HL behaves similarly as IgM617-HL with 2 main populations at 1166 +/- 21 kDa and 1052 +/- 34 kDa corresponding to hexamers (1035 kDa + 10 to 15%), and pentamers (862 kDa + 10 to 15%), but low oligomeric states can also be observed (Figures 2c).

Transmission Electron Microscopy

The structural integrity and oligomeric state of IgMs produced by HEK293F were examined and confirmed with negative staining Transmitted Electron Microscopy (TEM). IgM617-HLJ

(Figure 3b) and IgM012-HLJ (Figure 3d) produced in HEK293F exhibit very similar structural characteristics as previously observed for pentamers produced in HEK293E and CHO DG44, with a central circular core with projecting flexible Fab units in a star-shaped manner as well-known for IgMs isolated from human serum. As expected from biophysical data described above, IgM617-HL (Figure 3a) and IgM012-HL (Figure 3c) present distinct types of particles: some with an asymmetric shape to which five different arms can be attributed, some with a symmetric shape and six arms, confirming the hexameric structural features of HL samples in addition to the pentamer presence. As a remark, IgM molecules with lower oligomeric states observed with Mass Photometry and AUC could not be detected in TEM micrographs.

Taken together, our presented data confirmed that expression of pentameric IgM is possible in stable HEK293F cell lines and proteins with structural integrity can be purified from the culture supernatant. We also observed the formation of hexamers in addition to pentamers when only H and L chain genes are transfected to obtain stable HEK293F cells, but also to lesser extend the appearance of incomplete polymers. Nevertheless, in accordance with our observations using other cell lines, all of our results show that the retrieved production yields and protein quality differ significantly depending on individual recombinant IgM constructs, even when originated from culture media of HEK293F.

C1q-dependant complement activation by new IgM recombinant forms produced by HEK293F

The capacity of the new recombinant IgM preparations to activate CP was analyzed using our in-house *in vitro* Enzyme-Linked Immunosorbent Assay (ELISA) based on the detection of C4b fragment deposition after serum cleavage of C4 by the C1 complex bound to coated IgM molecules.[19,22] Assays with C1q-depleted normal human serum and C1q-reconstituted serum were used as controls for the C1q/IgM interaction dependency. Polyclonal IgMs purified from

human plasma (pIgMs) were used as positive control and standard. As observed with our previous IgM617 and IgM012 productions[22], no meaningful differences are observable in the C4b deposition yields regarding the coated recombinant IgM sample and they are comparable to the ones obtained with the coated serum-derived IgMs. Moreover, no differences are accountable to the presence of other IgM oligomeric states in IgM617-HL and IgM012-HL samples compared to the IgM pentamers IgM617-HLJ and IgM012-HLJ. Again, and as previously observed, the chemical differences introduced by the host cell, mainly polymer distributions, might not influence the ability of IgMs to activate the proteolytic complement cascade through C1 in these conditions (Figure 4).

C1q binding kinetics to IgMs measured by BLI

In order to characterize the binding kinetics of IgMs to C1q, we developed new protocols using a label-free optical method based on the Reflectometric Inference Spectroscopy (RIfS)[29,30] and its setup known as BioLayer Interferometry (BLI)[31,32] on an OctetRED96e instrument. During the course of this study, plasma purified C1q and plasma-derived IgM preparations and recombinant IgM constructs produced in HEK293F have been used as native reference and samples. In addition, we complemented our data with IgMs produced in CHO-DG44 and HEK293E from our previous studies.[22] Real-time detection of binding events at the surface of biosensors enables two strategies: (i) C1q can be captured as ligand at the biosensor surface and the IgM samples diluted in the analysis buffer and used as the analytes or (ii) the IgMs can be immobilized at the biosensor surface as ligands and C1q diluted in the analysis buffer and used as the analyte.

The first strategy has been evaluated with C1q as ligand either amine coupled onto AR2G biosensors or captured by Streptavidin (SA) biosensors after biotinylation. However, although high C1q densities can be reached (5 to 12 nm spectral shift), no or little binding responses can

be retrieved with IgM samples (data not shown).

The second strategy with IgMs captured on the biosensors has then been developed by testing different available methods and biosensors. Several commercial biosensors (AR2G, SA, APS, Protein A and Protein L) have first been evaluated for their abilities to capture IgM samples. Lab-made biosensors that are specific for capturing IgM were also prepared by saturating SA biosensors with either biotinylated mouse or goat anti-μ chain antibodies or CaptureSelect anti-IgM nanobody. Most types of biosensors can be functionalized at high levels with IgMs (between 1 to 7 nm spectral shift) except for Protein A biosensors which cannot bind IgM617 and IgM012 constructs. Protein A is specific to Fcγ regions of IgG but also to VH_3 subfamilies of Ig. IgM012 cannot be captured since its heavy variable region belongs to VH_1 family. Surprisingly, this is also true for IgM617 despite its VH_3 domain, while the biosensors can be easily functionalized with polyclonal IgMs. Unspecific binding of C1q was also evaluated for all biosensor types. Unfortunately, most of tested commercial biosensors (AR2G, Protein A, APS) without any loaded IgM showed strong unspecific signals of C1q, as previously reported by Zhou *et al.*.[18] At last, no C1q binding signal can be retrieved from most of the IgM-loaded biosensors (AR2G, SA, Protein A, APS). Only the protein L biosensors have shown to be suitable with limited C1q unspecific signals on the reference biosensors and measurable kinetics signals on the IgM-functionalized biosensors. Thus, pIgMs, IgM617 and IgM012 constructs were stably absorbed on Protein L biosensors until reaching saturation (5 to 7 nm shift). Kinetics analyses were then performed by dipping the IgM-functionalized biosensors in C1q concentration series ranging from 3.13 to 100 nM with 2-fold dilution (Figure 5).

All IgMs bind to C1q in a biphasic manner, with two distinguishable fast and slow binding rates, and the 1:1-Langmuir model could not be applied to determine interaction kinetics parameters. Thus, the only fitting model available to take into account both kinetics components

was the 2:1-heterogeneous-ligand model (Figure 5). Polyclonal IgMs extracted from plasma and all recombinant monoclonal IgMs show affinities in the nM scale, ranging from about 1 nM to 8nM for K_{D1} and from 4 to 26 nM for K_{D2}, depending on the sample (Table 1). Although the differences may not be significant, IgM012s seems to possess slightly better affinity for C1q (K_{D1} = 1 to 3 nM, K_{D2} = 4 to 10 nM) than IgM617s (K_{D1} = 6 to 8 nM, K_{D2} = 7 to 26 nM). They thus behave more similarly to pIgMs (K_{D1} = 2.3 nM, K_{D2} = 6.5 nM) than IgM617s. It has to be noted that for all IgM samples, both distinguishable slow and fast kinetics lead to affinities in the same nM order of magnitude. No significant differences in kinetics, which could be related to the host cell line, can be observed either for IgM617 or IgM012 models. Finally, although small differences can be noted in kinetics rate values when comparing HL and HLJ constructs, it is difficult to attribute them solely to the presence of hexameric forms, since such variations are also observed either between HLJ constructs or between preparations of the very same recombinant IgM construct (Table 1).

Discussion

In the presented study, we recombinantly produced and purified two IgMs models, IgM617 and IgM012[20–22] and to fully characterize their biochemical and functional quality using several biophysics techniques : (i) AUC, SEC-MALLS, MP and TEM to determine their oligomeric states and polymer distributions, (ii) *in vitro* complement activation based on ELISA to evaluate their functional capacities. Moreover, we developed a new method using a label-free and real-time detection technique, the BLI, to quantify the kinetics of the interaction between IgMs and the recognition and activating protein of the classical complement pathway, C1q.

One challenge for studying IgM and developing potential therapeutic products is the manufacturing of recombinant molecules of high quality in terms of Ig productivity, homogeneous oligomerization status, purity and biological biomimetic function. In the past

years, several methods have been tested and in particular both IgM617 and IgM012 have been taken as IgM models to develop proof-of-concepts of recombinant production.[20–23,25,33] Here, we supplemented the previous studies by presenting two additional stable productions of these models in HEK293F cells.

First, both IgMs were successfully produced as pentamers by transfecting the three H, L and J genetic constructs in HEK293F cells and generating stable cells. Transient expressions of both IgMs have been checked, but the resulting expression levels appeared either very low for IgM617-HLJ or undetectable for IgM012-HLJ (data not shown), suggesting slower intracellular and secretion processing by HEK293F strain than by the HEK293E strain used previously.[22] Also, as previously shown, large differences between IgM models in the finally retrieved yields of purified samples are observed.[22,26] Indeed, IgM012 expression and homogeneity still challenge HEK293F cells more than IgM617 production: IgM012-HLJ final yield remains very low or unretrievable compared to IgM617-HLJ, which can be produced and purified in large amounts. In the present study, we complemented biophysical sample analysis method panel by using SEC-MALLS (Supplemental Figure S1), sv-AUC (Supplemental Figure S2) and the new MP (Figure 2) to determine the oligomeric distribution of recombinant IgM samples. We can thus confirm that IgM617-HLJ model can be produced as very homogeneous pentamers when H, L and J chain genes are transfected in HEK293F for stable expression, while IgM012-HLJ retains heterogeneities with significant amount of lower oligomers. Despite these challenging behaviors, both IgM pentamers produced in HEK293F retain their structural integrity of five-branches-star-shaped particles (Figure 3) as shown with negative staining TEM images and functional qualities as demonstrated with complement activation assays (Figure 4). One explanation for the challenging behavior of IgM012 in recombinant expression compared to IgM617 and in general to other IgM constructs studied so far, may come from its origin: it is a class switch of the human monoclonal anti-HIV-1 antibody 2G12, one of the first and promising

neutralizing IgG discovered and characterized.[24] In addition, although the IgM012 pentamers produced in CHO cell line present enhanced potency of antiviral activity, our inability to produce this IgM construct in homogeneous form impairs its potential in therapeutic development. Structural determination of its IgG isoform has shown an unusual VH-VL domain arrangement for Fabs. Indeed, the 2G12 Fab crystal structure revealed that two of its Fabs assemble as a dimer with interlocked VH domain swapping, instead of the usual VH-VL monomeric assembly.[34] The VH domain exchange has been demonstrated to be mandatory for this IgG to target and to recognize the specific high-mannose cluster of the glycan shield of HIV-1.[35] One can easily hypothesize that IgM012 might possess such similar domain swapping of its Fabs and this might constrain IgM assembly more than the regular one in which Fabs behave independently. These structural constraints might not be favorable and might impair a proper expression of the IgM012 recombinant constructs by the different cell lines used so far.

With this study, we show that, by stably transfecting HEK293F cells with only the H and L constructs, IgM617-HL, and to a lesser extend IgM012-HL, hexamer expressions are made possible using HEK293F. It was well established that the J chain expression influences the formation of the pentameric and hexameric IgM forms either *in vivo* or *in vitro*. Randall *et al.* in 1992 first demonstrated the pentamer/hexamer ratio secretion regulation in B cells by J chain gene expression with the secretion of a majority of hexamers and a minority of pentamers by cells lacking the J chain gene.[36] However, recombinant expression of only hexamers by J-chain deficient cells remains challenging. Although hexamers were found to be expressed by recombinant systems, a majority of pentamers is found to be secreted by mouse hybridoma cell lines[37,38] or CHO-K1[39]. Interestingly, only Azuma *et al.* succeeded to obtain a majority of hexamers by using CHO-DG44 that expressed 20 times more hexamers that the CHO co-transfected with the J chain gene.[40] Here, we confirm that recombinantly producing homogeneous hexameric forms of IgM remains difficult. Although IgM617 and IgM012

models can be expressed and secreted as hexamers by stable HEK293F cell lines as shown by our different biochemical, biophysical and structural analyses, our data also show that both sample types are not homogeneous: they present a large population of pentamers likely lacking the J chain, but also traces of lower molecular weighted oligomers, likely tetramers and dimers, in the purified IgM samples. Moreover, the ratios between the distinct IgM oligomeric states appears not only variable from an IgM model to the other one but also between different productions of the same IgM model (data not shown). Additionally, our data from our surface-based C1q-dependent complement activation assays do not demonstrate higher activities of IgM samples enriched with hexamers (Figure 4). This contrasts with past hemolytic assays, which demonstrated the higher efficacy of hexameric IgM to induce complement-dependent cytolysis compared to pentameric IgMs.[38,41] As pointed previously, the ELISA-like setup and the end-point measurement of C4 deposition might not be sensitive and resolutive enough to characterize differences in IgM abilities to activate the first activation step of the complement.[22]

In this study and for the first time, we introduced a new method to characterize the binding kinetics and affinities of C1q to IgM antibody isotypes using BLI. Optical and surface-based methods such as SPR and BLI are popular methods to characterize the binding properties of all antibody classes to antigens, but much less to Ig effectors such as the complement molecule, C1q. Patel *et al.* in 2015[16] and Jovic *et al.* in 2019[42] have successfully characterized the binding responses of C1q to the different IgG subtypes using traditional SPR methods and Zhou *et al.* in 2018[18] using the recent BLI technology. Concerning the IgM/C1q interaction properties, a single study has been published by Bally *et al.* in 2019[19] who measured, using SPR, the binding kinetics between IgM fractions purified from human plasma and native C1q, as well as recombinant C1q and a few critical mutants.

Several experimental setups have been tested in our study to define the conditions allowing reliable binding measurements between either IgM purified from human plasma or different

recombinant IgM constructs and native C1q purified from human plasma. Surprisingly and in contrast to the SPR data obtained so far when C1q is captured at the biosensor surface[19], no interaction with IgMs was detectable with the BLI method. However, we could observe binding of the catalytic tetramer $C1r_2Cs_2$ to immobilized C1q with expected affinities in the nanomolar range (data not shown). These results indicate that immobilized C1q can retain certain binding activities towards its partners but that the immobilization strategy to the BLI biosensor either directly or via selective biotinylation of primary amines of C1q can greatly affect its binding capacities.

In the course of optimizing the BLI protocols, capturing IgMs on Protein L biosensor and using C1q as analyte has proven to be the most efficient strategy since only low or reasonable unspecific C1q binding can be detected at the used concentration range and specific concentration dependent binding signals can be measured (Figure 5). Our method meets the ones already employed to characterize the complex formation between C1q and recombinant IgGs, for which Protein L coated sensors have been used to capture immunoglobulins for SPR or BLI, although Streptavidin and biotin fusion have also been proven to be suitable.[18] Unfortunately, protein L was the only successful immobilization method for functionalizing BLI biosensors with IgMs. Indeed, it is known that binding of protein L to Igs is specifically restricted to certain kappa light chains, which limits the application of the method described here to IgMs containing this subtype of L chain, such as our models. Surprisingly, binding of C1q can be measured in those conditions and without any specific antigen bound to IgMs. Similarly, complement activation can be quantified without antigen with solid phase methods such as ELISA like techniques as shown by our presented and previous data[19,22], while antigen is required in solution methods such as erythrocyte or liposome lysis (for assays review in ref. 13). Indeed, it is thought that C1q binding to IgM, and subsequent complement cascade activation, are made possible only after IgM binding to specific antigen which induces large

structural changes in IgM quaternary structure and the exposure of the cryptic binding sites for C1q globular heads.[11] One possible explanation would be that immobilizing IgMs over an *in vitro* surface might somehow provoke the necessary structural feature exposures. In particular for BLI experiments for which only IgM captures via Protein L allow C1q binding, the explanation might come from the binding properties of Protein L to Ig. As shown by the 3D structure of the complex between Protein L and Fab, one Protein L domain bridges two Fab domains.[43] Although this property may not strictly mimic antigen binding, it might be enough to induce an IgM conformation allowing complex formation with C1q.

As expected, the measured affinities of C1q for IgMs with BLI fall within the nM range (Table 1). No significant differences in affinities and kinetics rates could be observed between polyclonal IgM purified from plasma and the different monoclonal recombinant IgMs. Together with the complement assays, which also show no differences between IgM samples, our BLI data emphasize that recombinant IgM preparations retain similar abilities as physiological IgMs to bind and to activate the CP *in vitro*. Our data are very consistent with SPR data obtained by Bally *et al.*.[19] However, the kinetics behavior appears to be different since a 2:1 heterogenous model has been applied to fit our BLI binding data (Figure 5), while a 1:1 Langmuir model is sufficient to interpret SPR data. One can argue that the biphasic kinetics behavior might be raised by the heterogenous quality of native or of our recombinant IgM samples. However, no difference is observed between the most homogeneous constructs (*i.e.* IgM617-HLJ) and the other ones. Thus, the differences observed between SPR and BLI data likely originate from the used methods and strategies: the used functionalized sensors have different capture chemistries and captured molecules (Amine coupled C1q in case of SPR, Protein L/IgMs in case of BLI) and different molecules are used as analyte (IgM in case of SPR, C1q in case of BLI). The question will remain unanswered since no binding could be detected with SPR, capturing IgMs on Protein L sensors and using C1q as analyte (data not shown). At last, BLI measurements of

the binding between IgMs and C1q might reveal intrinsic behaviors of the complex formation of those highly oligomeric and flexible molecules. It is expected that single globular region of C1q may have a lower affinity for Igs than full C1q, as well as IgM protomer for C1q than full IgM. Thus, the apparent and necessary affinities for the C1q/IgM complex formation rely on the specific multivalency that enhance the binding with an avidity effect. Furthermore, a certain liability of the C1q/Ig complex formation has been observed: not all gC1q bind the IgG hexamers at the same time[12], although the same behavior has not been described for IgMs[11]. Finally, because of the very high flexibility of IgM and C1q molecules, structural arrangements and stabilization are highly expected during the binding events. All taken together, these molecular characteristics would induce very complicated and heterogenous binding kinetics for which any mathematical fitting model would not be sufficiently formulated and easily applied to consider all possible behaviors.

As a conclusion, the development of biopharmaceuticals requires new *in vitro* methods to produce biosimilars and characterize the quality attributes of recombinant samples to meet the regulations of various drug and health authorities around the world. For antibodies, non-clinical studies must be performed to assess the similarity in known Fab- and Fc-associated functions such as binding to target antigen(s) and to Fc gamma receptors, FcRn and C1q. A particular challenge is to find methods to demonstrate the binding of Igs to C1q. For now, the characterization of this latter by ELISA have been widely used in pharmaceutical industry as a surrogate to complement dependent cytotoxicity assays in comparability studies for therapeutic Igs. Optical surface-based methods such as SPR and BLI have been proven to be alternatives with advantages like lower complexity in buffer preparations, lower hands-on manipulation, lower sample consumptions and to be faster, more in-depth and semi-automated IgG/C1q interaction analysis methods with higher precisions than the endpoint measurements from ELISA.[16,18,42] With our study, we demonstrated the suitability of the BLI-based assays for the

interaction of recombinant IgM/C1q interactions and we believe that the developed methods and protocols can be easily applied to evaluate future IgM potential therapeutical preparations in combination with the conventional biological analysis.

Materials and Methods

IgM genetic constructs

IgM617 is originally expressed by the EBV-transformed B cell line HB617 and directed against glycosphingolipids overexpressed on the tumor cell surfaces and elicit cytotoxic T-cells.[23] IgM012 was developed after a class switch of a human IgG broadly-neutralizing HIV and is directed against the HIV1 envelope protein gp120 and in particular the carbohydrate mannose structure.[24] All Light chains (L), Heavy chains (H) and Joining chain (J) cDNA of both IgM models were codon-optimized and sub-cloned into separate pIRES vectors as described in Chromikova *et al.*[25], into pCEP4 vectors as described in Hennicke *et al.*[20] and into pcDNA3.1(+) vectors. For the last constructs, IgM chain cDNAs were amplified by PCR using conventional protocols and the pIRES constructs as templates. Additional flanked NheI and BamHI restrictions sites were also introduced by Polymerase Chain Reaction (PCR). The genes were then inserted individually with classical ligation techniques into pcDNA3.1(+) vectors (Invitrogen) containing a resistance cassette for either Geneticin (H chain), Zeocin (L chain) or Hygromycin (J chain).

Cell lines and expression of IgM models

IgM617-HLJ and IgM012-HLJ forms were expressed using either (i) CHO DG44 cell lines after co-transfection with pIRES constructs and generation of stable cells lines as described in Chromikova *et al.*[25], (ii) HEK293E cell lines after co-transfection with pCEP4 vectors and transient expression as described in Hennicke *et al.*[21] or (iii) HEK293F after co-transfection or

serial transfections with pcDNA3.1(+) vectors and generation of stable cells lines.

Transfection and cultivation conditions of CHO DG44 and HEK293E cell lines have been described previously.[22,25] To generate stable IgM-expressing HEK293F cell lines, cells were grown in FreeStyle 293 expression medium and first co-transfected with H-chain- and L-chain-containing pcDNA3.1(+) plasmids using 293fectin according to the manufacturer's protocol (Invitrogen). Stable transfectants producing either IgM617-HL or IgM012-HL were generated using cultivation in medium supplemented with 400 µg/ml G418 (Invitrogen) and 10 µg/ml Zeocin (Invitrogen). These cells were then transfected with J-chain-containing pcDNA3.1(+) plasmids in the same way and the stable transfectants producing either IgM617-HLJ or IgM012-HLJ were generated using cultivation in medium supplemented with additional 100 µg/ml hygromycin (Sigma-Aldrich). The stable cells expressing each IgM construct were then expanded in Freestyle 293 expression medium under antibiotic pressures every 3 to 4 days when cell density approached 3.10^6 cells/ml.

Recombinant IgMs purification

All IgMs were purified from harvested supernatants according to Hennicke *et al.*[20]. Briefly, POROS CaptureSelect™ IgM Affinity Matrix (Thermo Fisher Scientific) was used for affinity chromatography. Culture supernatants were directly applied to packed column and the IgMs were eluted with 1 M Arginine, 2 M $MgCl_2$, pH 3.5 or pH 4.0. The collected fractions were immediately neutralized with 1M Tris pH 8.5. The IgM-containing fractions were then pooled and dialyzed against the next-step equilibration buffer. After concentration and for a second for Size Exclusion Chromatography (SEC) step, they were applied on a Superose™ 6 increase 10/300 or 16/600 columns (GE Healthcare/Cytiva) equilibrated in 0.1 M sodium phosphate pH 7.4, 0.2 M NaCl or in 0.025 M Tris-Base, 0.137 M NaCl, 0.003 M KCl, pH7.4 at a flow rate of 0.5 mL/min. Highly multimeric IgMs were eluted as a single peak separated from lower or

higher oligomeric states and from nucleic acid contaminants. Identification of purified IgMs by SDS-PAGE was performed as described in Vorauer-Uhl *et al.*[23] using Native PAGE 3-12% Bis-Tris gels and followed by Coomassie Blue staining.

C1q purification from plasma

C1q was purified from human serum according to the well-established protocol published by Arlaud *et al.*.[44]

Analytical Ultracentrifugation

Sv-AUC experiments were conducted in an XLI analytical ultracentrifuge (Beckman, Palo Alto, CA) using an ANTi-60 rotor and double channel Ti centre pieces (Nanolytics, Germany) of 12- or 3-mm optical path length equipped with sapphire windows, the reference channel being typically filled with the sample solvent. Acquisitions were done overnight at 4°C and at 20000rpm (32000g) using absorbance (280 nm) and interference detection. Data processing and analysis were done using the program SEDFIT[45] from P. Schuck (NIH, USA), REDATE[46] and GUSSI[47] from C. Brautigam (USA), and using standard equations and protocols described in refs. 48–50.

Size Exclusion Chromatography - Multi Angle Laser Light scattering (SEC-MALLS) analyses

SEC combined with online detection by MALLS, refractometry and UV-Vis was used to measure the absolute molecular mass in solution. The SEC runs were performed using a Superose™ 6 increase 10/300 column (GE Healthcare/Cytiva) equilibrated in 0.025 M Tris-Base, 0.137 M NaCl, 0.003 M KCl, pH 7.4. Separation was performed at room temperature and 50 µl of protein sample, concentrated to about 1 mg/ml, were injected with a constant flow rate of 0.5 ml/min. Online MALLS and differential refractive index detection were performed with

respectively a DAWN-HELEOS II detector (Wyatt TechnologyCorp.) using a laser emitting at 690 nm and an Optilab T-rEX detector (Wyatt Technology Corp.), respectively. Weight-averaged molar masses (Mw) determination was done with the ASTRA6, using the "protein conjugate" module of the ASTRA software package. The following refractive index increments and UV-Vis absorbance values were used: *dn/dc* protein = 0.185 mL/g; *dn/dc* glycosylation = 0.15 mL/g; A_{280}=1.38 ml/mg.cm.

Mass Photometry

Coverslips (high precision glass coverslips, 24x50 mm^2, No. 1.5H; Marienfeld, Lauda-Königshofen, Germany) were cleaned by sequential sonication in Milli-Q H_2O, 50% iso-propanol (HPLC grade)/Milli-Q H_2O, and Milli-Q H_2O (5 min each), followed by drying with a clean nitrogen stream. To keep the sample droplet in shape, reusable self- adhesive silicone culture wells (Grace Bio-Labs reusable CultureWell™ gaskets) were cut in segments of 4 to 10. To ensure proper adhesion to the coverslips, the gaskets were dried well by using a clean nitrogen stream. To prepare a sample carrier, gaskets were placed in the center of the cleaned coverslip and fixed tightly by applying light pressure with the back of a pipette tip. Protein landing was recorded using a Refeyn One^{MP} (Refeyn Ltd., Oxford, UK) MP system by forming a droplet of each IgM sample with a final concentration of 10 nM in a buffer solution containing 0.025 M Tris-Base, 0.137 M NaCl, 0.003 M KCl, pH7.4. Movies were acquired for 120 s (12000 frames) with Acquire^{MP} (Refeyn Ltd., v2.1.1) software using standard settings. Contrast-to-mass (C2M) calibration was performed using a mix of proteins with molecular weight of 66, 146, 500, and 1046 kDa. Data were analyzed using Discover^{MP} (Refeyn LTD, v2.1.1) and analysis parameters were set to T1 = 1.2 for threshold 1. The values for number of binned frames (nf = 8), threshold 2 (T2 = 0.25), and median filter kernel (=15) remained constant. The mean peak contrasts were determined in the software using Gaussian fitting. The mean contrast values were then plotted and fitted to a line. The experimental masses were

finally obtained by averaging replicates and errors were the standard deviation.

Transmission electron microscopy (TEM)

About 4 µl of diluted IgM samples (60 to 80 ng) were applied to a carbon film evaporated onto a mica sheet. The carbon film was then floated off the mica in ~100 µL 2 % sodium silicotungstate (SST, Agar Scientific) and transferred onto a 400 mesh Cu TEM grid (Delta Microscopies). Images were acquired with a CETA camera on a Tecnai F20 TEM microscope operating at 200 keV.

Complement activation-ELISA

The activation of the classical complement pathway was monitored by an ELISA based on the detection of C4b deposition according to Bally *et al.* and Hennicke *et al.*.[19,22] In brief, 200 ng of IgMs were immobilized on a MaxiSorp 96-well plate (Thermo Fisher Scientific) and incubated with Normal Human Serum (NHS) diluted 25 times, C1q-depleted serum (NHSΔ, CompTech) diluted 25 times or NHSΔ diluted 25 times reconstituted with purified human C1q (4 µg/mL). NHS was obtained from the Etablissement Français du Sang Rhône-Alpes (agreement number 14-1940 regarding its use in research). Unspecific binding was prevented by saturation with 2% bovine serum albumin (BSA, Sigma Aldrich). Deposited cleaved C4 form was detected with a rabbit anti-human C4 polyclonal antibody (Siemens), an anti-rabbit-HRP antibody conjugate (Sigma Aldrich), addition of TMB (Sigma Aldrich) and a Clariostar plate reader (BMG Labtech). Polyclonal IgM isolated from human serum (Sigma Aldrich) was used as control. Reported values were obtained by normalizing each data set (polyclonal IgM/NHS defined as 100) and by averaging them obtained in replicated independent assays (between 2 to 4); Reported errors were the standard deviation of the replicates.

BioLayer Interferometry

All BLI experiments were performed on an OctetRED96e from Pall/FortéBio and were recorded with the manufacturer software (Data Acquisition v11.1). All protein samples were buffer exchanged against 0.01 M Na_2HPO_4, 0.0018 M KH_2PO_4, 0.137 M NaCl, 0.0027 M KCl at pH 7.4 (Phosphate Buffer Saline, PBS) or 0.025 M Tris, 0.15 M NaCl, 0.003 M KCL at pH 7.4 (Tris Buffer Saline, TBS) with Zeba Spin Desalting columns (Thermo Fisher Scientific) prior to any loading. In the course of testing and optimization, AR2G (amine coupling), SA (streptatividin), APS (aminopropylsilane), Protein A and Protein L biosensors were used. Lab-made IgM-specific biosensors were also prepared as following: Mouse or goat anti-μ chain antibodies (Invitrogen) or CaptureSelect anti-IgM nanobody (Thermo Fisher Scientific) were biotinylated using NHS-PEG4-biotin EZ-link kit (Thermo Fisher Scientific) and manufacturer conditions, then captured onto SA biosensors. For loading on AR2G biosensors, IgM samples were diluted in 0.01 M Sodium Acetate at pH 4, 4.5, 5, 5.5 or 6 and C1q in either 0.01 M Sodium Acetate at pH 4, 4.5, 5 or 5.5, 0.01 M MES at pH 6 or 6.5 or 0.01 M HEPES at pH 7 or 7.5; for loading on SA biosensor, IgM and C1q samples were biotinylated using NHS-PEG4-biotin EZ-link kit (Thermo Fisher Scientific) and manufacturer conditions; no chemical treatments were applied before loading on APS, Protein A, Protein L or lab-made biosensors. All ligand samples were finally diluted at concentrations between 10 and 50 μg/ml. For association and dissociation, all analyte samples were diluted at concentration between 10 and 100 nM in TBS complemented with 0.002 M $CaCl_2$ and 0.02% Tween-20 as analysis buffer. 0.2 ml of each sample or buffer were disposed in wells of black 96-well plates (Nunc F96 MicroWell, Thermo Fisher Scientific), maintained at 25°C and agitated at 1000 rpm the whole time. Prior to each assay, all biosensors were pre-wetted in 0.2 ml PBS, 0.02% Tween-20 or analysis buffer for 10 min, followed by equilibration in pre-wetting buffer for 120 s. Biosensors were then loaded with each ligand prepared according to the capture chemistry for 600 s,

followed by an additional equilibration step of 120 s in analysis buffer. Association phases were monitored during dipping the functionalized biosensors in analyte solutions for between 180 s and 300 s, and the dissociation phases monitored in analysis buffer for between 180 s and 300 s. To assess and monitor analyte unspecific binding, blank biosensors were treated in the same but replacing the ligand solution by analysis buffer. Kinetics analyses were performed using Protein L biosensors which were functionalized with each IgM sample diluted at 30 µg/ml for 600 s until reaching a spectrum shift between 5.5 and 7.0 nm. Association phase of plasma C1q was monitored for 300 s with concentrations between 0 and 100 nM and dissociation phase for 600 s. All measurements were performed in duplicates with independent IgM loadings. Kinetics data were processed with the manufacturer software (Data analysis HT v11.1). Signals from blank biosensor and zero-concentration sample were subtracted from the signals obtained for each functionalized biosensor and each analyte concentration. Resulting specific kinetics signals were then fitted using a global fit method and 2:1 heterogeneous ligand model. Reported kinetics parameter values were obtained by averaging the values obtained with replicated assays (between 2 to 4) and reported errors as the standard deviation.

Acknowledgements

cDNA coding for IgM617 and IgM012 chains were provided by Polymun Scientific Immunobiologische Forschung GmbH. This work used the Biophysical, AUC, EM and SPR/BLI platforms of the Grenoble Instruct-ERIC center (ISBG; UAR 3518 CNRS-CEA-UGA-EMBL) within the Grenoble Partnership for Structural Biology (PSB), supported by FRISBI (ANR-10-INBS-0005-02) and GRAL, financed within the University Grenoble Alpes graduate school (Ecoles Universitaires de Recherche) CBH-EUR-GS (ANR-17-EURE-0003). We thank Caroline Mas for her assistance at the Biophysical platform, Christine Ebel and Aline Le Roy at AUC platform. The EM facility is supported by the Auvergne Rhône-Alpes Region,

the Fondation pour la Recherche Médicale (FRM), the Fonds FEDER and the GIS-Infrastructures en Biologie Santé et Agronomie (IBiSA). We thank Guy Schoehn, head of EM facility, for his support. IBS acknowledges integration into the Interdisciplinary Research Institute of Grenoble (IRIG, CEA). We would like to thank Véronique Rossi and Christine Gaboriaud from IBS for their expertise, helpful discussions and article proof reading.

Funding details

This work was supported by the French National Research Agency under Grant C1qEffero ANR-16-CE11-0019, the PhD program BioToP (Biomolecular Technology of Proteins) funded by the FWF under Grant W1224 and by Polymun Scientific Immunobiologische Forschung GmbH (Julia Hennicke's Ph.D. Thesis).

Disclosure statement

The authors declare that they have no conflicts of interest with the contents of this article.

Abbreviations

AUC: Analytical Ultra-Centrifugation

BLI: BioLayer Interferometry

CLR: Collagen-like region of C1q

ELISA: Enzyme-Linked Immunosorbent Assay

H/H chain: Heavy chain

L/L chain: Light chain

gC1q: globular head of C1q

Ig/Igs: Immunoglobuline/s

IgG/IgGs: Immunoglobuline/s G

IgM/IgMs: Immunoglobuline/s M

J/J chain: Joining chain

ELISA: Enzym-Linked Immunosorbent Assay

EM: Electron Microscopy

MP: Mass Photometry

PCR: Polymerase Chain Reaction

RIfS: Reflectometric Interference Spectroscopy

SEC: Size Exclusion Chromatography

SEC-MALLS: Multi-Angle-Light Scattering coupled to Size Exclusion Chromatography

SPR: Surface Plasmon Resonance

TEM: Transmitted Electron Microscopy

PAGE: PolyAcrylamide Gel Electrophoresis

References

1. Jones K, Savulescu AF, Brombacher F, Hadebe S. Immunoglobulin M in Health and Diseases: How Far Have We Come and What Next? Front. Immunol. 2020;11:doi:10.3389/fimmu.2020.595535.
2. Gong S, Ruprecht RM. Immunoglobulin M: An Ancient Antiviral Weapon – Rediscovered. Front. Immunol. 2020;11:1943. doi:10.3389/fimmu.2020.01943.
3. Keyt BA, Baliga R, Sinclair AM, Carroll SF, Peterson MS. Structure, Function, and Therapeutic Use of IgM Antibodies. Antibodies 2020;9:53. doi:10.3390/antib9040053.
4. Hiramoto E, Tsutsumi A, Suzuki R, Matsuoka S, Arai S, Kikkawa M, Miyazaki T. The IgM pentamer is an asymmetric pentagon with an open groove that binds the AIM protein. Sci. Adv. 2018;4:eaau1199. doi:10.1126/sciadv.aau1199.
5. Li Y, Wang G, Li N, Wang Y, Zhu Q, Chu H, Wu W, Tan Y, Yu F, Su X-D, et al. Structural insights into immunoglobulin M. Science 2020;367:1014–1017. doi:10.1126/science.aaz5425.
6. Kumar N, Arthur CP, Ciferri C, Matsumoto ML. Structure of the human secretory immunoglobulin M core. Structure 2021;S0969212621000022. doi:10.1016/j.str.2021.01.002.

7. Ricklin D, Hajishengallis G, Yang K, Lambris JD. Complement - a key system for immune surveillance and homeostasis. Nat. Immunol. 2010;11:785–797. doi:10.1038/ni.1923.
8. Cedzyński M, Thielens NM, Mollnes TE, Vorup-Jensen T. Editorial: The Role of Complement in Health and Disease. Front. Immunol. 2019;10:1869. doi:10.3389/fimmu.2019.01869.
9. Kishore U, Reid KBM. C1q: Structure, function, and receptors. Immunopharmacology 2000;49:159–170. doi:10.1016/S0162-3109(00)80301-X.
10. Diebolder CA, Beurskens FJ, de Jong RN, Koning RI, Strumane K, Lindorfer MA, Voorhorst M, Ugurlar D, Rosati S, Heck AJR, et al. Complement Is Activated by IgG Hexamers Assembled at the Cell Surface. Science 2014;343:1260–1263. doi:10.1126/science.1248943.
11. Sharp TH, Boyle AL, Diebolder CA, Kros A, Koster AJ, Gros P. Insights into IgM-mediated complement activation based on in situ structures of IgM-C1-C4b. Proc. Natl. Acad. Sci. 2019;201901841. doi:10.1073/pnas.1901841116.
12. Ugurlar D, Howes SC, de Kreuk B-J, Koning RI, de Jong RN, Beurskens FJ, Schuurman J, Koster AJ, Sharp TH, Parren PWHI, et al. Structures of C1-IgG1 provide insights into how danger pattern recognition activates complement. Science 2018;359:794–797. doi:10.1126/science.aao4988.
13. Harboe M, Thorgersen EB, Mollnes TE. Advances in assay of complement function and activation. Adv. Drug Deliv. Rev. 2011;63:976–987. doi:10.1016/j.addr.2011.05.010.
14. Duncan AR, Winter G. The binding site for C1q on IgG. Nature 1988;332:738. doi:10.1038/332738a0.
15. Idusogie EE, Presta LG, Gazzano-Santoro H, Totpal K, Wong PY, Ultsch M, Meng YG, Mulkerrin MG. Mapping of the C1q Binding Site on Rituxan, a Chimeric Antibody with a Human IgG1 Fc. J. Immunol. 2000;164:4178–4184. doi:10.4049/jimmunol.164.8.4178.
16. Patel R, Neill A, Liu H, Andrien B. IgG subclass specificity to C1q determined by surface plasmon resonance using Protein L capture technique. Anal. Biochem. 2015;479:15–17. doi:10.1016/j.ab.2015.03.012.
17. Moore GL, Chen H, Karki S, A G. Engineered Fc variant antibodies with enhanced ability to recruit complement and mediate effector functions. mAbs 2010;2:181–189. doi:10.4161/mabs.2.2.11158.

18. Zhou W, Lin S, Chen R, Liu J, Li Y. Characterization of antibody-C1q interactions by Biolayer Interferometry. Anal. Biochem. 2018;549:143–148. doi:10.1016/j.ab.2018.03.022.
19. Bally I, Inforzato A, Dalonneau F, Stravalaci M, Bottazzi B, Gaboriaud C, Thielens NM. Interaction of C1q with pentraxin 3 and IgM revisited: mutational studies with recombinant C1q variants. Front. Immunol. 2019;10:461. doi:10.3389/fimmu.2019.00461.
20. Hennicke J, Lastin AM, Reinhart D, Grünwald-Gruber C, Altmann F, Kunert R. Glycan profile of CHO derived IgM purified by highly efficient single step affinity chromatography. Anal. Biochem. 2017;539:162–166. doi:10.1016/j.ab.2017.10.020.
21. Hennicke J, Reinhart D, Altmann F, Kunert R. Impact of temperature and pH on recombinant human IgM quality attributes and productivity. New Biotechnol. 2019;50:20–26. doi:10.1016/j.nbt.2019.01.001.
22. Hennicke J, Schwaigerlehner L, Grünwald-Gruber C, Bally I, Ling WL, Thielens N, Reiser J-B, Kunert R. Transient pentameric IgM fulfill biological function—Effect of expression host and transfection on IgM properties. PLOS ONE 2020;15:e0229992. doi:10.1371/journal.pone.0229992.
23. Vorauer-Uhl K, Wallner J, Lhota G, Katinger H, Kunert R. IgM characterization directly performed in crude culture supernatants by a new simple electrophoretic method. J. Immunol. Methods 2010;359:21–27. doi:10.1016/j.jim.2010.05.003.
24. Wolbank S, Kunert R, Stiegler G, Katinger H. Characterization of Human Class-Switched Polymeric (Immunoglobulin M [IgM] and IgA) Anti-Human Immunodeficiency Virus Type 1 Antibodies 2F5 and 2G12. J. Virol. 2003;77:4095–4103. doi:10.1128/JVI.77.7.4095-4103.2003.
25. Chromikova V, Mader A, Steinfellner W, Kunert R. Evaluating the bottlenecks of recombinant IgM production in mammalian cells. Cytotechnology 2015;67:343–356. doi:10.1007/s10616-014-9693-4.
26. Chromikova V, Mader A, Hofbauer S, Göbl C, Madl T, Gach JS, Bauernfried S, Furtmüller PG, Forthal DN, Mach L, et al. Introduction of germline residues improves the stability of anti-HIV mAb 2G12-IgM. Biochim. Biophys. Acta 2015;1854:1536–1544. doi:10.1016/j.bbapap.2015.02.018.
27. Eskeland T, Christensen TB. IgM Molecules with and without J Chain in Serum and after Purification, Studied by Ultra-centrifugation, Electrophoresis, and Electron

Microscopy. Scand. J. Immunol. 1975;4:217–228. doi:10.1111/j.1365-3083.1975.tb02620.x.

28. Sonn-Segev A, Belacic K, Bodrug T, Young G, VanderLinden RT, Schulman BA, Schimpf J, Friedrich T, Dip PV, Schwartz TU, et al. Quantifying the heterogeneity of macromolecular machines by mass photometry. Nat. Commun. 2020;11:1772. doi:10.1038/s41467-020-15642-w.
29. Hänel C, Gauglitz G. Comparison of reflectometric interference spectroscopy with other instruments for label-free optical detection. Anal. Bioanal. Chem. 2002;372:91–100. doi:10.1007/s00216-001-1197-3.
30. Gauglitz G. Critical assessment of relevant methods in the field of biosensors with direct optical detection based on fibers and waveguides using plasmonic, resonance, and interference effects. Anal. Bioanal. Chem. 2020;412:3317–3349. doi:10.1007/s00216-020-02581-0.
31. Abdiche Y, Malashock D, Pinkerton A, Pons J. Determining kinetics and affinities of protein interactions using a parallel real-time label-free biosensor, the Octet. Anal. Biochem. 2008;377:209–217. doi:10.1016/j.ab.2008.03.035.
32. Sultana A, Lee JE. Measuring Protein-Protein and Protein-Nucleic Acid Interactions by Biolayer Interferometry. Curr. Protoc. Protein Sci. 2015;79:19.25.1-19.25.26. doi:10.1002/0471140864.ps1925s79.
33. Mader A, Chromikova V, Kunert R. Recombinant IgM expression in mammalian cells: A target protein challenging biotechnological production. Adv. Biosci. Biotechnol. 2013;04:38–43. doi:10.4236/abb.2013.44A006.
34. Calarese DA, Scanlan CN, Zwick MB, Deechongkit S, Mimura Y, Kunert R, Zhu P, Wormald MR, Stanfield RL, Roux KH, et al. Antibody Domain Exchange Is an Immunological Solution to Carbohydrate Cluster Recognition. Science 2003;300:2065–2071. doi:10.1126/science.1083182.
35. Doores KJ, Fulton Z, Huber M, Wilson IA, Burton DR. Antibody 2G12 Recognizes Di-Mannose Equivalently in Domain- and Nondomain-Exchanged Forms but Only Binds the HIV-1 Glycan Shield if Domain Exchanged. J. Virol. 2010;84:10690–10699. doi:10.1128/JVI.01110-10.
36. Randall TD, Parkhouse RM, Corley RB. J chain synthesis and secretion of hexameric IgM is differentially regulated by lipopolysaccharide and interleukin 5. Proc. Natl. Acad. Sci. U. S. A. 1992;89:962–966. doi:10.1073/pnas.89.3.962.

37. Wiersma EJ, Collins C, Fazel S, Shulman MJ. Structural and Functional Analysis of J Chain-Deficient IgM. J. Immunol. 1998;160:5979–5989. .

38. Collins C, Tsui FWL, Shulman MJ. Differential activation of human and guinea pig complement by pentameric and hexameric IgM. Eur. J. Immunol. 2002;32:1802–1810. doi:10.1002/1521-4141(200206)32:6<1802::AID-IMMU1802>3.0.CO;2-C.

39. Gilmour JEM, Pittman S, Nesbitt R, Scott ML. Effect of the presence or absence of J chain on expression of recombinant anti-Kell immunoglobulin M. Transfus. Med. 2008;18:167–174. doi:10.1111/j.1365-3148.2008.00853.x.

40. Azuma Y, Ishikawa Y, Kawai S, Tsunenari T, Tsunoda H, Igawa T, Iida S, Nanami M, Suzuki M, Irie RF, et al. Recombinant Human Hexamer-Dominant IgM Monoclonal Antibody to Ganglioside GM3 for Treatment of Melanoma. Clin. Cancer Res. 2007;13:2745–2750. doi:10.1158/1078-0432.CCR-06-2919.

41. Randall TD, King LB, Corley RB. The biological effects of IgM hexamer formation. Eur. J. Immunol. 1990;20:1971–1979. doi:10.1002/eji.1830200915.

42. Jovic M, Cymer F. Qualification of a surface plasmon resonance assay to determine binding of IgG-type antibodies to complement component C1q. Biologicals 2019;61:76–79. doi:10.1016/j.biologicals.2019.08.004.

43. Graille M, Stura EA, Housden NG, Beckingham JA, Bottomley SP, Beale D, Taussig MJ, Sutton BJ, Gore MG, Charbonnier J-B. Complex between Peptostreptococcus magnus Protein L and a Human Antibody Reveals Structural Convergence in the Interaction Modes of Fab Binding Proteins. Structure 2001;9:679–687. doi:10.1016/S0969-2126(01)00630-X.

44. Arlaud GJ, Sim RB, Duplaa A-M, Colomb MG. Differential elution of Clq, C$\bar{1}$r and C$\bar{1}$s from human CT bound to immune aggregates. use in the rapid purification of C$\bar{1}$ sub-components. Mol. Immunol. 1979;16:445–450. doi:10.1016/0161-5890(79)90069-5.

45. Schuck P. Size-Distribution Analysis of Macromolecules by Sedimentation Velocity Ultracentrifugation and Lamm Equation Modeling. Biophys. J. 2000;78:1606–1619. doi:10.1016/S0006-3495(00)76713-0.

46. Zhao H, Ghirlando R, Alfonso C, Arisaka F, Attali I, Bain DL, Bakhtina MM, Becker DF, Bedwell GJ, Bekdemir A, et al. A Multilaboratory Comparison of Calibration Accuracy and the Performance of External References in Analytical Ultracentrifugation. PLoS ONE 2015;10:e0126420. doi:10.1371/journal.pone.0126420.

47. Brautigam CA. Chapter Five - Calculations and Publication-Quality Illustrations for Analytical Ultracentrifugation Data. *Methods in Enzymology* 2015;109–133. doi:10.1016/bs.mie.2015.05.001.

48. Le Roy A, Nury H, Wiseman B, Sarwan J, Jault J-M, Ebel C. Sedimentation Velocity Analytical Ultracentrifugation in Hydrogenated and Deuterated Solvents for the Characterization of Membrane Proteins. in*Membrane Biogenesis: Methods and Protocols* (eds. Rapaport, D. & Herrmann, J. M.) (Humana Press, 2013).;219–251. doi:10.1007/978-1-62703-487-6_15.

49. Le Roy A, Wang K, Schaack B, Schuck P, Breyton C, Ebel C. Chapter Twelve - AUC and Small-Angle Scattering for Membrane Proteins. in*Methods in Enzymology* (ed. Cole, J. L.) (Academic Press, 2015).;vol. 562:257–286. doi:10.1016/bs.mie.2015.06.010.

50. Salvay AG, Santamaria M, le Maire M, Ebel C. Analytical Ultracentrifugation Sedimentation Velocity for the Characterization of Detergent-Solubilized Membrane Proteins Ca++-ATPase and ExbB. J. Biol. Phys. 2008;33:399. doi:10.1007/s10867-008-9058-3.

Figure legends

Figure 1. Semi-native PolyAcrylamide Gel Electrophoresis (PAGE) analysis of purified IgMs samples from HEK293F expression. Native PAGE gels followed by Coomassie Blue staining were run to identify IgM617-HLJ and IgM617-HL (a) and IgM012-HLJ and IgM012-HL (b) polymer distributions after SEC purification. IgM purified from plasma (Antibodies-onlines) are taken as makers along with Native Markers. Suspected hexamers (H), pentamers (P), dimers (D) and monomers (M) are indicated with arrows.

Figure 2. Mass Photometry analysis of recombinant IgMs produced in HEK293F. Histograms show the population distributions of purified IgMs. Shown analyses are representative of replicate experiments: IgM617-HL (a), IgM617-HLJ (b), IgM012-HL (c) and IgM012-HLJ (d). Estimated molecular weights for the shown experiments are indicated on each graph.

Figure 3. Non-processed images of negative stain transmission electron microscopy images of recombinant IgMs produced in HEK293F. Representative fields of particles with a 50 nm scale bar on top of each panel and magnified views of some individual molecules are shown on the

lower part of each panel: IgM617-HL (a), IgM617-HLJ (b), IgM012-HL (c), IgM012-HLJ (d). Hexamers are denoted with H and Pentamers with P.

Figure 4. Complement activation by the different purified IgMs constructs expressed in HEK293F. Recombinant IgMs and IgMs purified from plasma were coated on microplate wells and incubated with either Normal Human Serum (NHS), C1q-depleted NHS (NHSΔ) or reconstituted NHS (NHSΔ + C1q). C1 activity was monitored via C4b deposition. Reported values are average of replicated (2 to 4) and normalized experiments (100% = IgM plasma/NHS). Errors are obtained as standard deviation between independent replicates.

Figure 5. Kinetics analysis of the interaction between C1q from plasma and the different purified and immobilized full IgMs expressed in mammalian expression hosts. IgMs were captured on Protein L and functionalized biosensors were dipped in wells containing C1q at different concentrations (0, 3.13, 6.25, 12.5, 25, 50, 100 nM). The binding signals (grey-scaled sensorgrams) were obtained by subtracting the signals from empty protein L biosensor and from zero-concentration samples. Fitted curved are depicted as black lines and were obtained by global fitting using a 2:1 heterogenous ligand model. Shown kinetics analysis are representative of each binding experiment: IgM012-HLJ expressed by CHO DG44 (a), IgM617-HLJ by CHO DG44 (b), IgM012-HLJ by HEK293E (c), IgM617-HLJ by HEK293E (d), IgM012-HLJ by HEK293F (e), IgM617-HLJ by HEK293F (f), IgM012-HL by HEK293F (g), IgM617-HL by HEK293F (h), IgMs purified from plasma (i).

Table

Table 1. Kinetics and affinity constants of C1q binding to the different purified recombinant IgMs expressed in mammalian expression systems. Values are obtained after global fitting of the binding signals (see Figure 5) and averaging from replicates (2 to 4). Affinity constants (K_{D1} and K_{D2}) are obtained from the ratio between kinetics parameters (k_{d1}/k_{a1} and k_{d2}/k_{d1}). Standard errors are obtained as standard deviation between replicates.

IgM	Source	Oligomers	k_{a1} 10^5/Ms	k_{d1} 10^{-4}/s	**K_{D1} 10^{-9} M**	k_{a2} 10^7/Ms	k_{d2} 10^{-1}/s	**K_{D2} 10^{-9} M**
Total IgM	**plasma**		3.04 ± 0.47	7.02 ± 1.63	**2.31 ± 0.09**	2.00 ± 0.90	1.30 ± 0.60	**6.52 ± 1.34**
IgM617	**CHO DG44**	**HLJ**	0.78 ± 0.17	6.20 ± 1.02	**8.00 ± 0.31**	0.57 ± 0.44	0.74 ± 0.08	**12.30 ± 3.87**
	HEK293E	**HLJ**	0.92 ± 0.16	6.26 ± 1.77	**6.82 ± 0.11**	0.86 ± 0.49	0.59 ± 0.33	**6.90 ± 1.13**
	HEK293F	**HLJ**	1.59 ± 0.76	11.30 ± 3.04	**7.10 ± 1.06**	0.44 ± 0.05	1.15 ± 0.53	**26.4 ± 2.89**
	HEK293F	**HL**	1.66 ± 0.50	9.25 ± 4.84	**5.59 ± 1.02**	0.96 ± 0.38	0.96 ±0.47	**9.97 ± 2.00**
IgM012	**CHO DG44**	**HLJ**	2.22 ± 0.08	2.57 ± 0.37	**1.16 ± 0.01**	2.04 ± 0.31	1.34 ± 0.13	**6.54 ± 0.11**
	HEK293E	**HLJ**	1.64 ± 0.35	3.57 ± 0.33	**2.18 ± 0.06**	1.84 ± 0.40	1.57 ± 0.15	**8.51 ± 0.24**
	HEK293F	**HLJ**	2.22 ± 0.33	6.18 ± 0.08	**2.79 ± 0.03**	1.41 ± 0.34	1.34 ± 0.28	**9.50 ± 0.48**
	HEK293F	**HL**	4.65 ± 2.54	5.81 ± 2.61	**1.25 ± 0.31**	1.79 ± 0.51	0.73 ± 0.04	**4.09 ± 0.17**

Figure 1

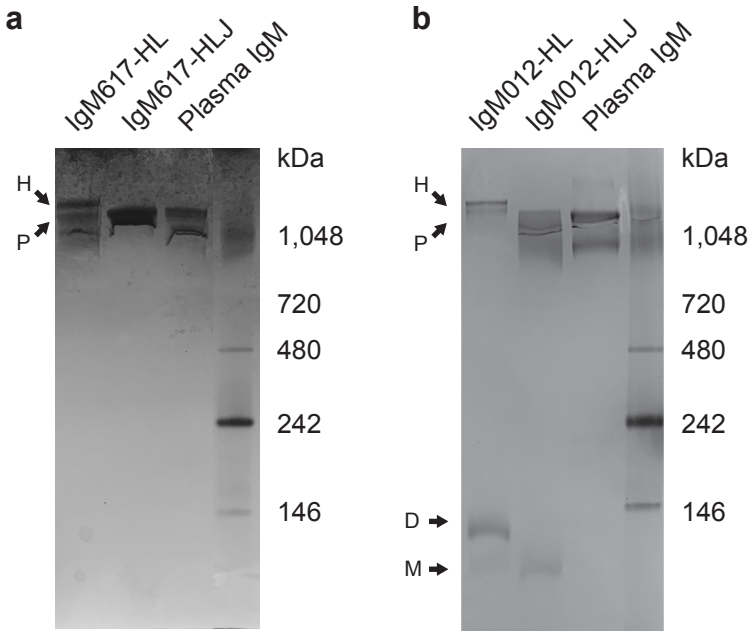
a
IgM617-HL
IgM617-HLJ
Plasma IgM
kDa
H
P
1,048
720
480
242
146
b
IgM012-HL
IgM012-HLJ
Plasma IgM
kDa
H
P
1,048
720
480
242
146
D
M

Figure 2

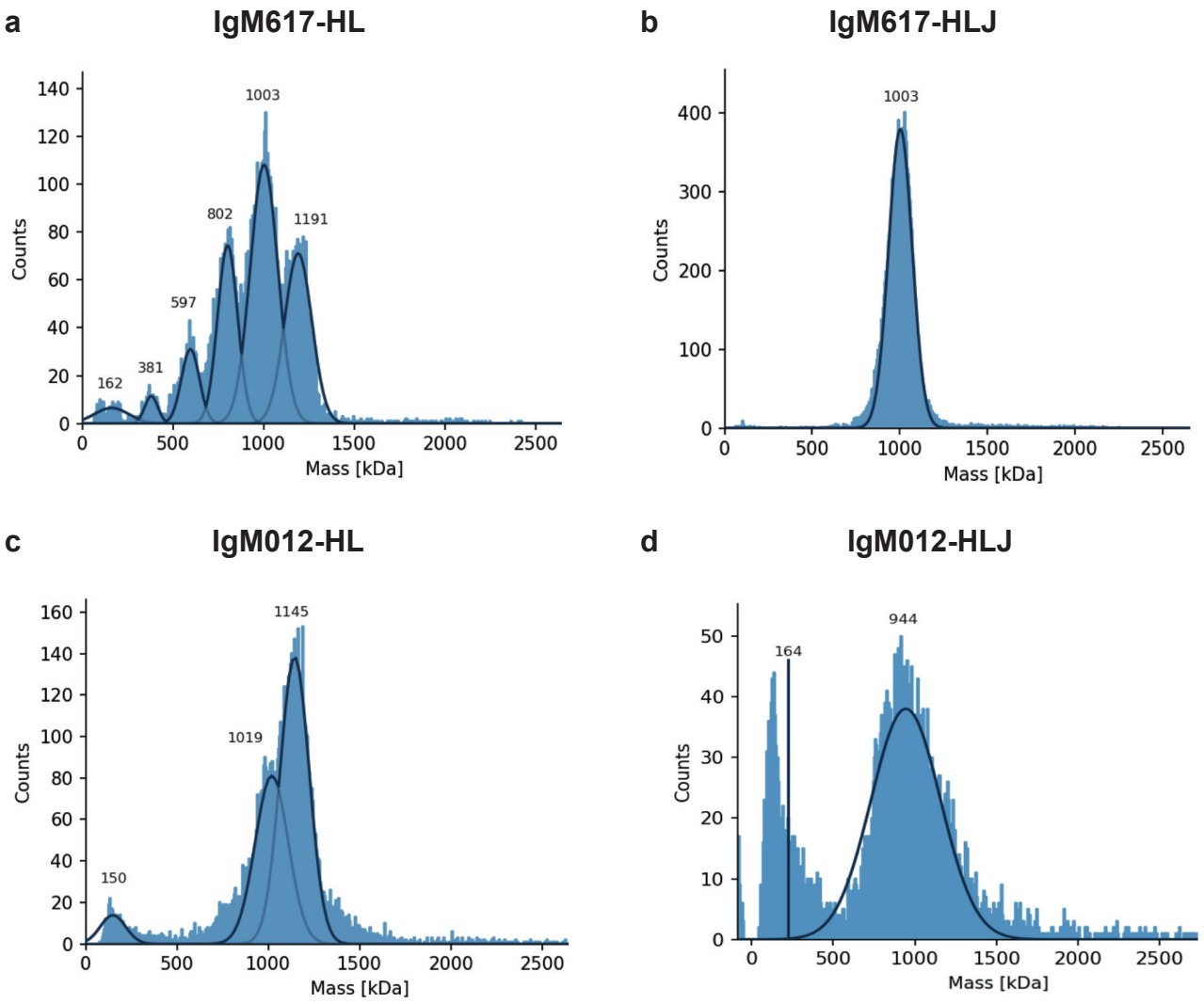
a
IgM617-HL
Counts
Mass [kDa]
162
381
597
802
1003
1191
b
IgM617-HLJ
Counts
Mass [kDa]
1003
c
IgM012-HL
Counts
Mass [kDa]
150
1019
1145
d
IgM012-HLJ
Counts
Mass [kDa]
164
944

Figure 3

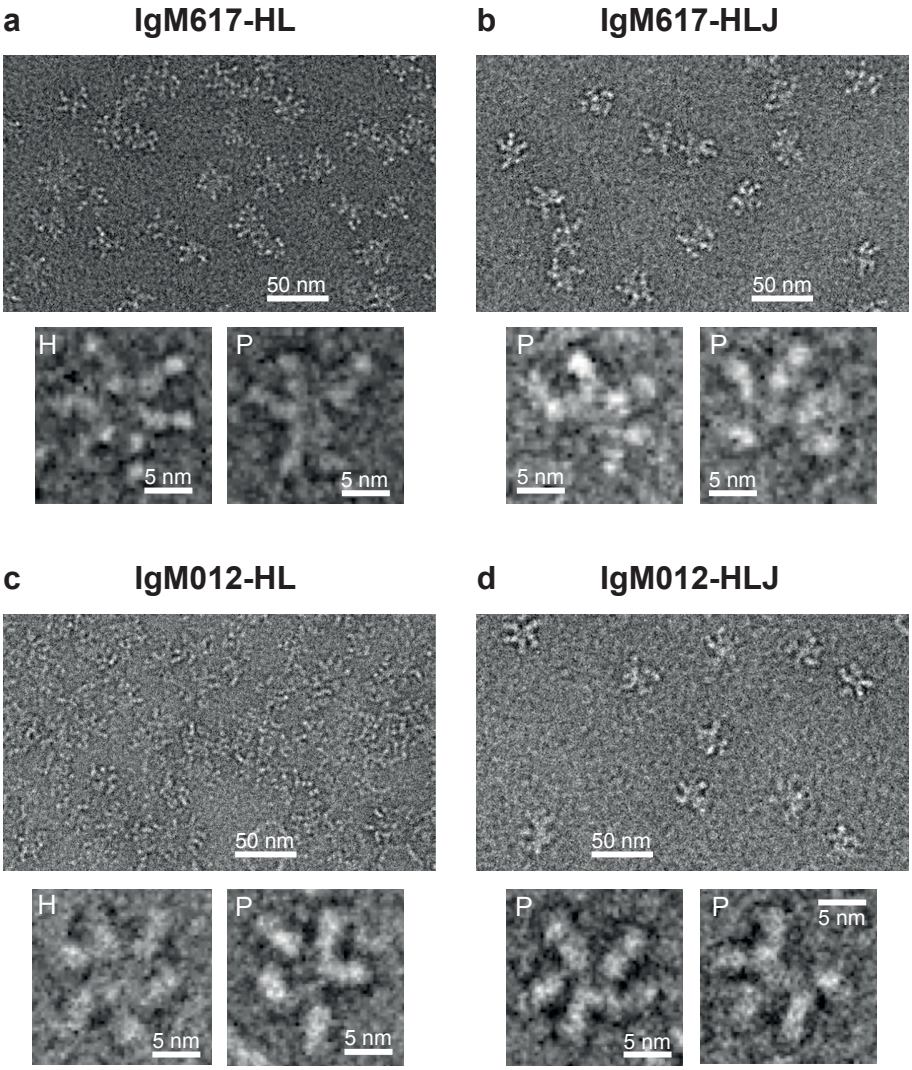
a
IgM617-HL
50 nm
H
5 nm
P
5 nm
b
IgM617-HLJ
50 nm
P
5 nm
P
5 nm
c
IgM012-HL
50 nm
H
5 nm
P
5 nm
d
IgM012-HLJ
50 nm
P
5 nm
P
5 nm

Figure 4

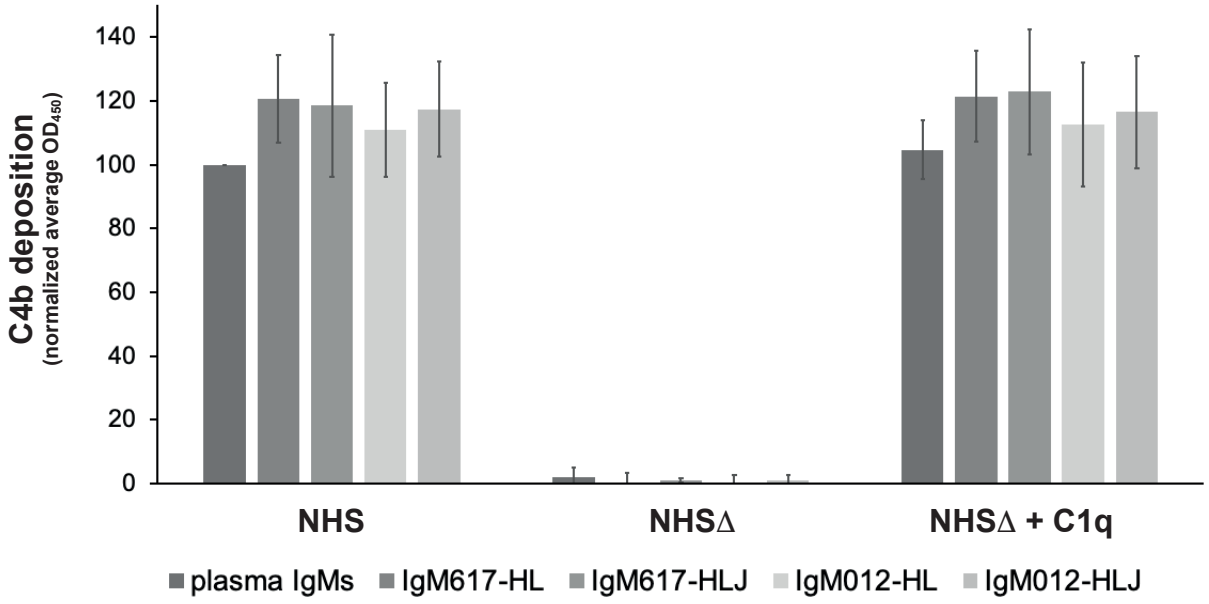
C4b deposition
(normalized average OD450)
140
120
100
80
60
40
20
0
NHS
NHSΔ
NHSΔ + C1q
plasma IgMs
IgM617-HL
IgM617-HLJ
IgM012-HL
IgM012-HLJ

Figure 5

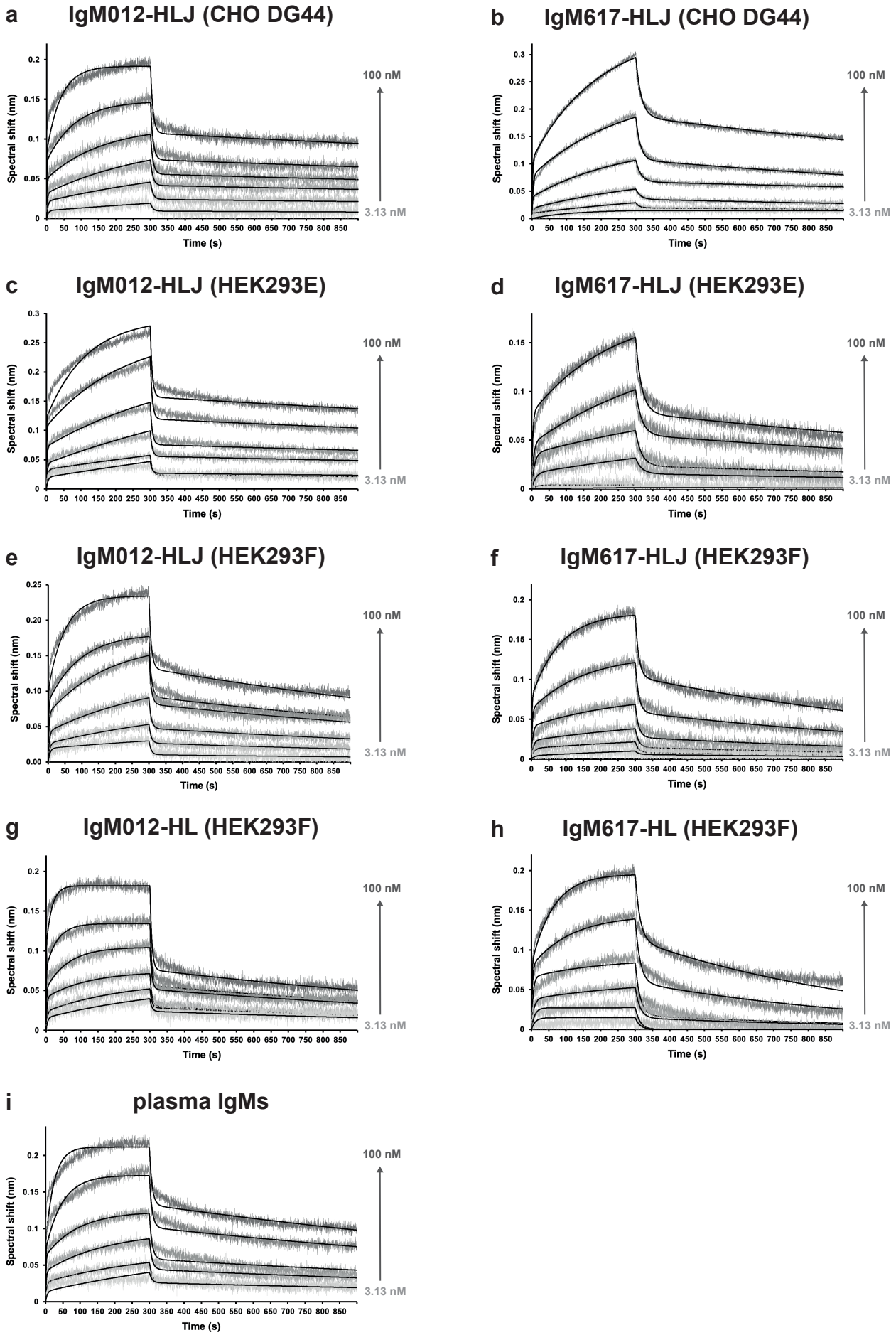
a
IgM012-HLJ (CHO DG44)
b
IgM617-HLJ (CHO DG44)
c
IgM012-HLJ (HEK293E)
d
IgM617-HLJ (HEK293E)
e
IgM012-HLJ (HEK293F)
f
IgM617-HLJ (HEK293F)
g
IgM012-HL (HEK293F)
h
IgM617-HL (HEK293F)
i
plasma IgMs
Spectral shift (nm)
Time (s)
100 nM
3.13 nM